8th International Conference on Photonic Technologies LANE 2014

The application of specific point energy analysis to laser cutting with 1 µm laser radiation

M. Hashemzadeh[a], W.Suder[b], S. Williams[b], J.Powell[c], A.F.H. Kaplan[c], K.T. Voisey[a]*

a. Faculty of Engineering, University of Nottingham, NG7 2RD, UK.
b.Welding Engineering Research Centre, Cranfield University, MK43 0AL, UK.
c. Dept. of Eng. Sciences and Mathematics, Luleå University of Technology, S-971 87 Luleå, Sweden

Abstract

Specific point energy (SPE) is a concept that has been successfully used in laser welding where SPE and power density determine penetration depth. This type of analysis allows the welding characteristics of different laser systems to be directly compared. This paper investigates if the SPE concept can usefully be applied to laser cutting. In order to provide data for the analysis laser cutting of various thicknesses of mild steel with a 2kW fibre laser was carried out over a wide range of parameter combinations. It was found that the SPE concept is applicable to laser cutting within the range of parameters investigated here.

Selection and blind-review under responsibility of the Bayerisches Laserzentrum GmbH.

Keywords: fibre laser cutting; power density; parameter analysis, specific point energy

1. Introduction

Fibre laser cutting is widely used in industry to cut sheet metal, most commonly steel with thicknesses of a few millimetres[1-4]. There is a lot of interest on how to determine the optimum parameter combination for a given cutting scenario. A large body of published work exists in which various parameters are varied systematically in order to find the optimum combination. This approach is used for all laser material processing techniques[5-7], including laser cutting[8-12]. The effects of changing laser power, traverse speed, focal spot size and power density on the process are well documented. It is also widely known that it is useful to consider the combined term P/V, power/velocity, in such analyses[13]. However, the majority of such work considers only one laser system and in practice the four parameters listed above are interlinked and cannot be completely decoupled. Whilst there are similarities of observed trends from one system to another, results cannot be directly compared.

Recently Suder et al. [14] presented laser welding results which involved the novel analysis approach of specific point energy (SPE). The work showed that three basic laser material interaction parameters: power density, interaction time and specific point energy, allow the welding process to be defined regarding the depth of penetration and weld width.

1.1. Specific point energy analysis

The basic parameters relevant to laser material processing are power density ρ_P, interaction time T_i, and the beam dimensions where it meets the workpiece. The average power density ρ_P, of a laser beam, is given by Equation 1, where P is laser power and A is the laser spot area on the sheet surface.

$$\rho_P = \frac{P}{A} \qquad (1)$$

For a point on the centre line of a circular cross section beam with a spot diameter d moving at a speed V the interaction time T_i is given by Equation 2. As a first approximation this can be taken as the interaction time between the laser and the material (in practice the interaction time is progressively smaller as we move away from the centreline of the circular beam).

* Corresponding author. Tel.: +44-115-951-4139
E-mail address: katy.voisey@nottingham.ac.uk

$$T_i = \frac{d}{V} \qquad (2)$$

The average energy density, i.e. the average energy delivered per unit area, is the product of power density and interaction time and is given by Equation 3.

$$\rho_E = \rho_P T_i = \frac{Pd}{AV} \qquad (3)$$

It is important to note that the same energy density can be generated with different beam sizes. Hence, additional information is required to fully specify the laser processing conditions. The energy delivered to the material in the interaction time of $\boldsymbol{T_i}$, termed specific point energy (S_{PE}) by Suder et al. [14], can be calculated by Equation 4. Suder et al. [14] demonstrated that the laser welding process can be fully characterised by reference to both the power density and specific point energy.

$$S_{PE} = \rho_P T_i A = PT_i = \frac{Pd}{V} \qquad (4)$$

It is worth highlighting that results from the systematic variation of individual parameters, as well as the effects of simultaneously changing more than one parameter, can be explained in terms of SPE. Figure 1 demonstrates that a change in power density from 1.6 MW cm^{-2} to 0.4 MW cm^{-2} could be achieved by either decreasing the laser power or increasing the spot size. If, for example, we take the welding situation described at point 1 on the graph and double the laser spot diameter, the energy density would drop from 1.6MW cm^{-2} to 0.4 MW cm^{-2} resulting in a move from point 1 to point 2 on the graph (decreasing the depth of penetration from 5 to 3 mm). However, this is counteracted by an increase in the interaction time because of the increase in spot size. This increases the SPE, and results in an automatic shift from point 2 to point 3 (increasing the depth of penetration from 3 to 4 mm). So doubling the laser beam diameter from the conditions described in point 1 of the graph results in a decrease in depth of penetration from 5mm to 4mm.

The work of Suder et al. [14] showed that the depth of penetration is controlled by the power density and the SPE but the weld width is controlled by the interaction time [14, 15] (see Figure 1b). The aim of this paper is to determine if this type of approach can also be used for laser cutting and to determine how individual parameters effect the key, industrially relevant, cutting features of kerf width, cutting cost and cutting efficiency.

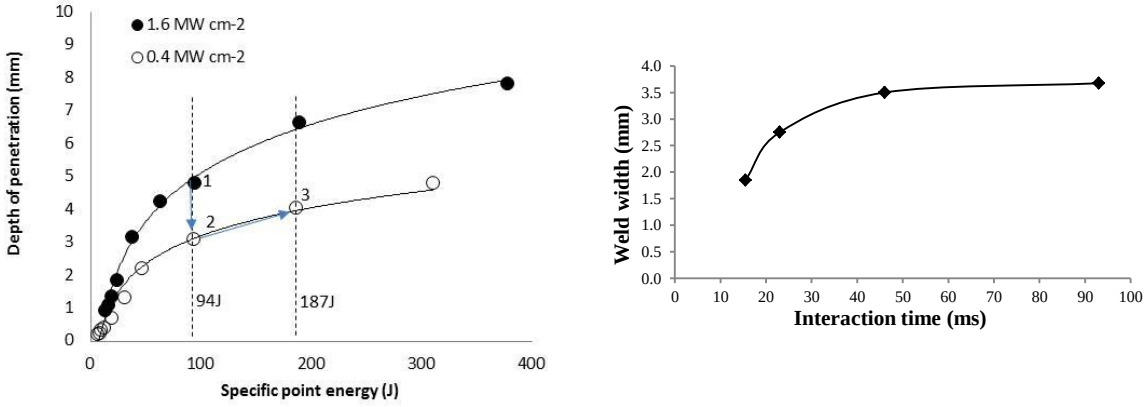

(a) (b)

Figure 1 Key results from Suder et al. [14] (a) Variation of depth of weld penetration as a function of specific point energy (b) Variation of weld width with interaction time for weld penetration depth of 6 mm achieved with a 0.75mm beam diameter and a range of power-velocity combinations [15].

2. Experimental methods

Cold rolled mild steel with thicknesses of 1, 2, 3, 4 and 6 mm was used throughout this work. The material to be cut was clamped to an x-y table and traversed under the laser head. The cut line was positioned above a hollow gully so that molten material and gas could exit the rear of the cut material without any hindrance. All laser cutting was carried out with an IPG YLR-2000 ytterbium fibre laser with a maximum power of 2 kW and a 1.06 μm wavelength. 12 bar gauge pressure nitrogen was used

as an assist gas for all cuts, delivered via a 1 mm diameter nozzle with a 1 mm stand off distance. Throughout the work the focal plane of the laser was set to coincide with the upper surface of the cut sheet.

Two different focal length lenses were used: 120 mm and 80 mm. These were used the three delivery fibres, with diameters of 600 μm, 400 μm and 200 μm to produce the five optical set ups detailed in Table 1. The focused beam diameters reported were measured using a Primes focus monitor. It should be noted that these measurements were made at a power of 600 W for the 120 mm lens and 400 W for the 80 mm. There is a slight variation in beam diameter with power, for the 400 μm fibre when used with the 80 mm lens the beam diameter increased by less than 2% when power increased from 400 W to 600 W. The five different optical set ups were combined with the parameters detailed in Table 2 to generate the 106 different parameter combinations for which results are reported.

Table 1 Measureed focussed beam diameters for the five optical set ups used

Focal length (mm)	Delivery fibre (μm)	Focussed beam diameter (mm)
120	200	0.20
120	400	0.37
120	600	0.60
80	200	0.15
80	400	0.26

Table 2 Parameter ranges

Parameter	Values
Velocity (mm min^{-1})	90 - 7200
Power (W)	120-1672

An important difference between laser welding and laser cutting is that in cutting it is generally the case that a portion of the beam passes through the laser-material interaction zone. This is because the cut front inclination varies with speed, being near vertical at low speeds where, as shown in Figure.2a, part of the laser beam may pass straight through the cut without interacting with the material. At higher speeds the cut front becomes less perpendicular, increasing the proportion of the beam that interacts with the material (Figure.2a) but in any case a proportion of the beam is reflected off the cut front. By using maximum cutting speeds, as has been done for all results presented in this paper, it can be assumed that there is sufficient cut front inclination to make any straight-through losses negligible. This was done by incrementally decreasing power until a through cut was no longer obtained. Figure.2b shows the precision to which this cut/no cut power boundary was determined, as can be seen, in each case the maximum cut speed was established to within 5-10%.

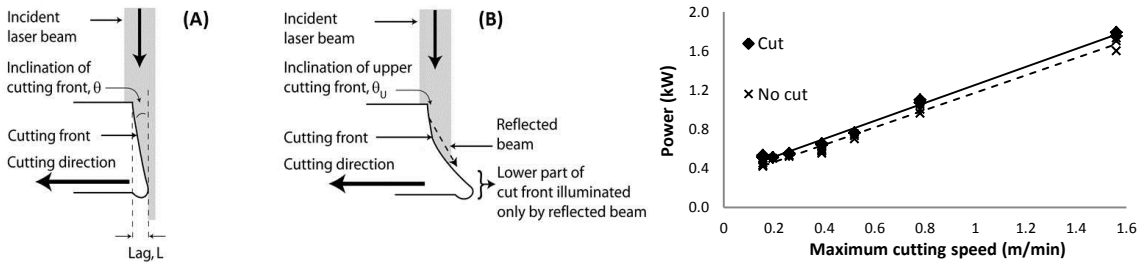

Figure.2- Showing cut front laser beam interaction geometries. (A) Slower cutting speed (steep cut front, some laser beam is lost), (B) Faster cutting speed (less steep cut front, all laser beam interacts with cut edge) [16] (B) Confirmation of the maximum cut speeds measured during these experiments, results shown for 4 mm sheet thickness, 0.26 mm beam diameter.

Kerf width measurements were made with a Keyence VHX-100 optical microscope, the results presented are the average of three measurements all taken from the central region of the cut in order to avoid any effects due to initial acceleration or deceleration of the table during the start and end of the cut.

3. Results

3.1. Application of specific point energy analysis to laser cutting

Figure 3 displays the power density for each of the 106 cuts produced, with the samples ordered in ascending power density. In order to determine if SPE analysis can be applied to cutting an attempt was made to replicate the depth of penetration/SPE

graph from Suder et al. [14] (presented as earlier as Figure 1a). This required the identification of groups of results with similar power densities. The groups selected are highlighted in Figure 3. In each case the results refer to a maximum speed cut for the laser set up/material combination involved and so these results can be interpreted as either maximum speed for the material thickness or as maximum thickness for the speed involved (see figure 2b). If the results are taken as 'maximum thickness' then a graph analogous to Suder et al.'s [14] 'depth of penetration' results can be produced – as presented in figure 4.

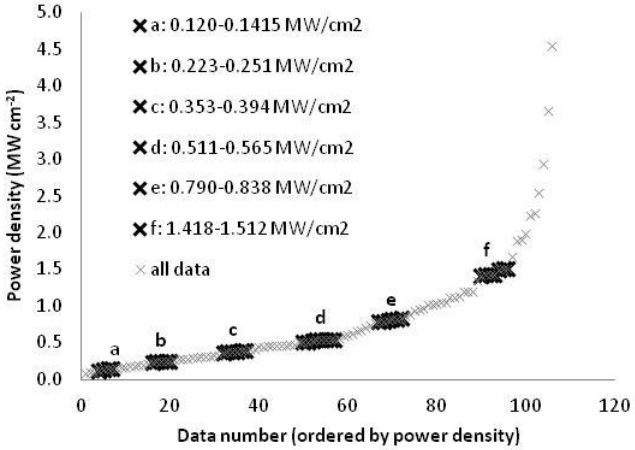

Figure 3 Grouping of data by power density

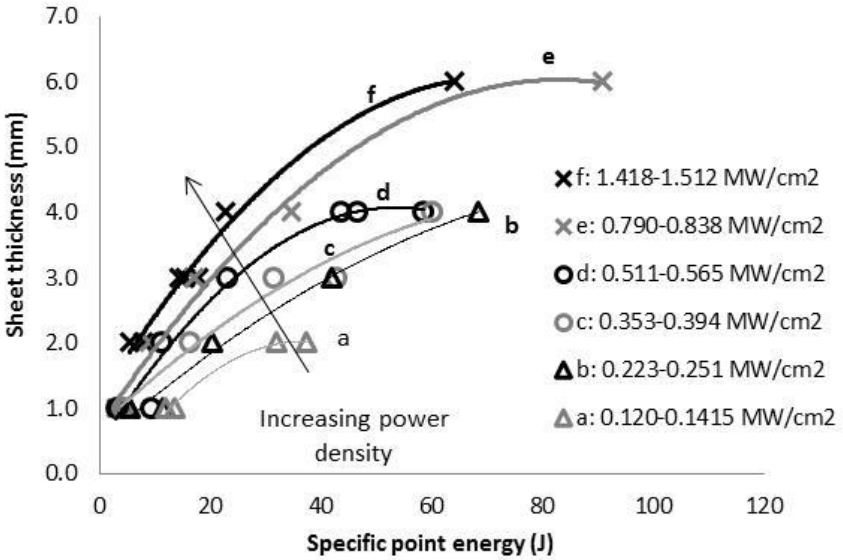

Figure 4 Maximum cut sheet thickness (for the parameters used in each case) plotted as a function of specific point energy for the power density data sets identified in Figure 3.

From the SPE for cuts in different thickness sheets at different power densities, as shown in Figure 4, it can be seen that:

1. The same thickness can be cut by decreased SPE and increased power density. For example, with the same power and a decrease in the beam diameter, the cutting speed is increased, boosting the cutting efficiency.
2. With the same SPE, the maximum cut sheet thickness can be increased by increasing power density.
3. With the same power density, the maximum cut sheet thickness increases with increasing SPE.

3.2. Kerf width

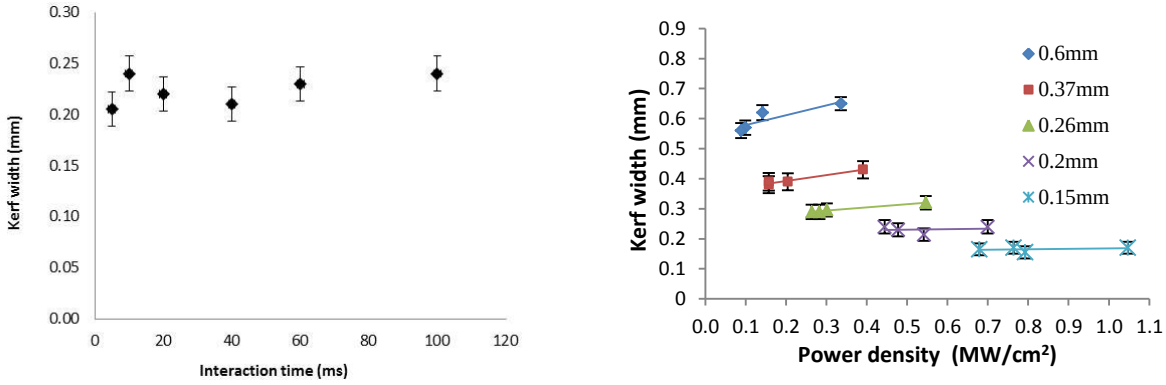

(a) (b)

Figure 5 Kerf width results for cutting of 1 mm sheet thickness (a) 0.2 mm beam diameter results plotted versus interaction time for different power-velosity combinations (b) kerf width plotted versus power for different beam diameters.

It was mentioned earlier that Suder et al. [14] identified a link between interaction time and width of weld produced. The 'width of weld' is analogous to the 'kerf width' in laser cutting but in this case (as figure 5a, for example, demonstrates) there is a minimal correlation between kerf width and interaction time. However, the kerf width does vary significantly with beam size (Figure 5b).

For each beam diameter an increase in kerf width with power density can be seen in Figure 5b, with the absolute size of the variation increasing with beam diameter. This effect is attributed to the beam not having a perfect top hat power distribution. As the power density of increases for a given nominal beam size the effective cutting diameter of the beam increases because the edges of the beam profile are not perfectly perpendicular, as illustrated in Figure 6. As the power of the beam is increased the diameter of the beam which exceeds the energy density threshold for melting the material also increases. Thus, higher powers produce wider cut kerfs.

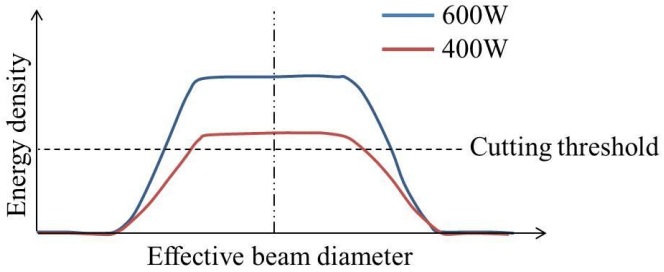

Figure 6 Schematic illustrating how region of beam exceeding a given threshold varies with power.

4. Discussion

A comparison of Figure 1 and Figure 4 shows that SPE analysis is applicable to laser cutting within the parameters used in this study. This means that results from different optical set ups, and ultimately from different laser systems, could be directly compared.

This work has highlighted a key difference between cutting and welding. In welding the weld width was previously reported as being mainly controlled by interaction time, for a given weld penetration depth [14, 15], whereas the results in Figure 5 show that in laser cutting of a given thickness the kerf width is mainly controlled by the beam diameter. This difference is due to the fact that in cutting lateral conduction of heat is severely limited by the continual removal of molten material from the cutting zone. This essentially acts as a cooling process, removing thermal energy from the kerf before any significant lateral conduction takes place. However, in welding there is no such material removal so all the thermal energy input from the laser beam remains in the workpiece and is available to conduct laterally and extend the width of the molten region.

In order to usefully exploit this new analysis tool the relationships between SPE and cutting cost and efficiency will now be

considered as these are two factors of great interest to industrial laser cutting.

One of the main costs of laser cutting is that of the energy used in the process. For a given cut length the energy input is simply the laser power divided by the speed. A plot of this energy used per length of cut against SPE (Figure 7a) shows that the data falls on a series of straight lines, with each line starting at the origin. Further consideration shows that the plot of power/speed, against SPE, ((power × beam diameter)/speed) would be expected to produce a set of straight lines with the gradient of each line corresponding to 1/beam diameter. This is clearly seen in Figure 7b where data point markers correspond to beam diameter. It is clear from these results that, within the parameters used in these tests, a larger beam diameter leads to a reduction in energy used per meter of cut.

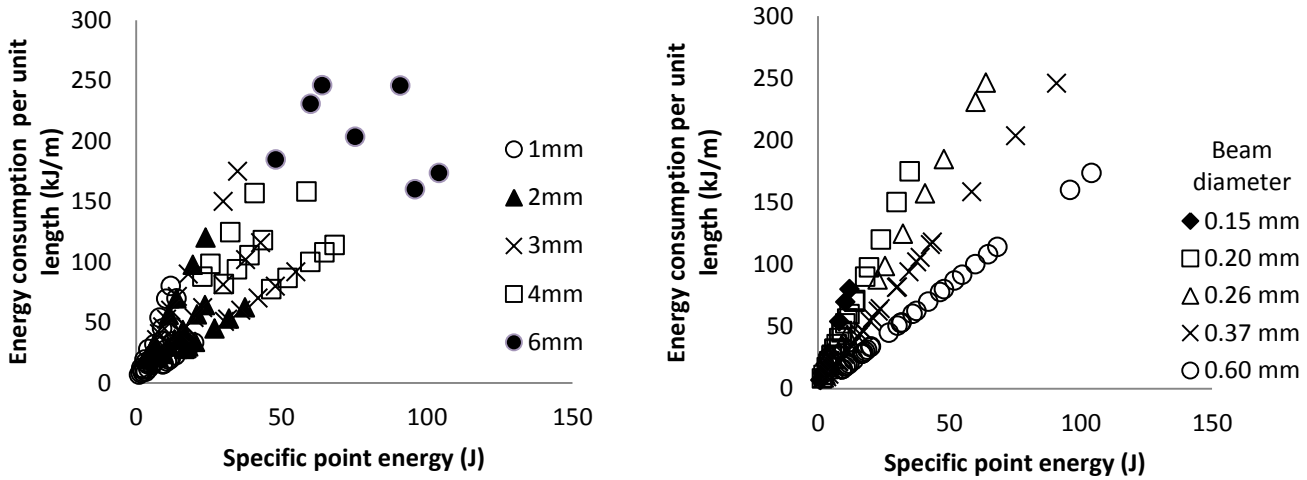

(a) (b)

Figure 7 Energy used per length of cut plotted against SPE showing that data forms straight lines, (a) data point markers correspond to material thickness (b) data point markers correspond to different beam diameters.

The analysis can also be expanded to include cutting efficiency. Cutting efficiency, C_{eff}, is defined here as the ratio of the area of cut surface generated per second to the energy input from the laser per second:
C_{eff} = ((sheet thickness × length cut per second) / energy input per second) = ((sheet thickness × speed) / power)

In Figure 8 where results from all thicknesses are plotted, the cutting efficiency is seen to increase with decreasing SPE, but there is a lot of scatter in the data and no trend relating to power density is discernable.

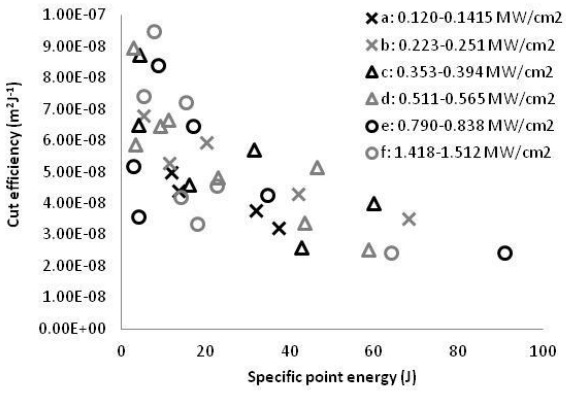

Figure 8 Variation of cutting efficiency with SPE for all thicknesses, markers indicate power density range of data.

However, in Figure 9, where a single material thickness is considered, the cut efficiency results, when plotted against SPE, clearly fall onto discrete lines according to beam diameter.
Again, further consideration reveals that such plots would be expected to produce discrete lines of the form $y=1/x^2$ corresponding

to different beam diameters since C_{eff} = ((sheet thickness × speed) / power)) and SPE = (beam diameter × power) / speed.

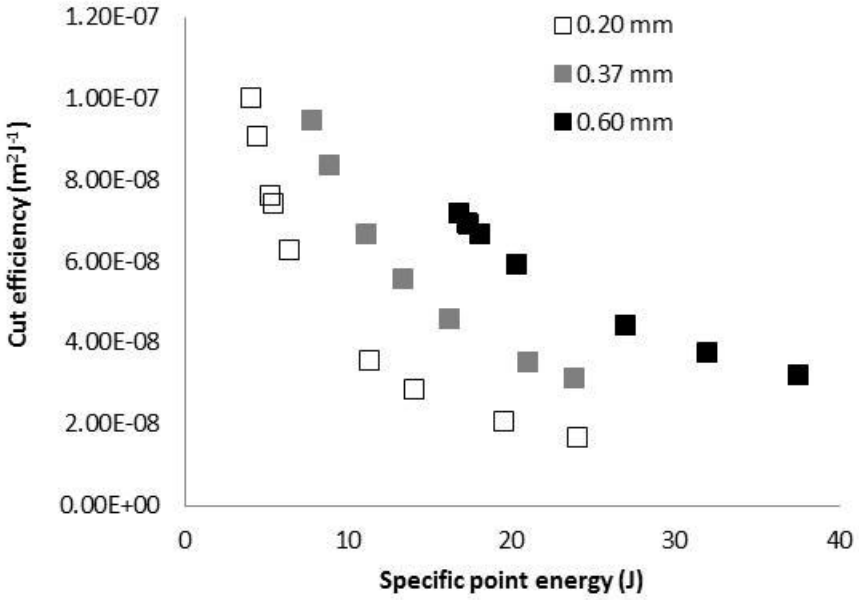

Figure 9 Cutting efficiency results for 2 mm cuts plotted against SPE, data markers indicate different beam diameters.

Optimal laser cutting will have high efficiency and low cost, i.e. it will have a high value of C_{eff}/C_{cost}. Equation 5 shows that for a given material thickness, t, this ratio is proportional to $(V/P)^2$ so this the factor (The Cutting Optimisation Parameter) should be maximised to optimise cutting as long as the cut quality is acceptable.

$$\frac{C_{eff}}{C_{cost}} = \frac{tV/P}{P/V} = t\left(\frac{V}{P}\right)^2 \qquad (5)$$

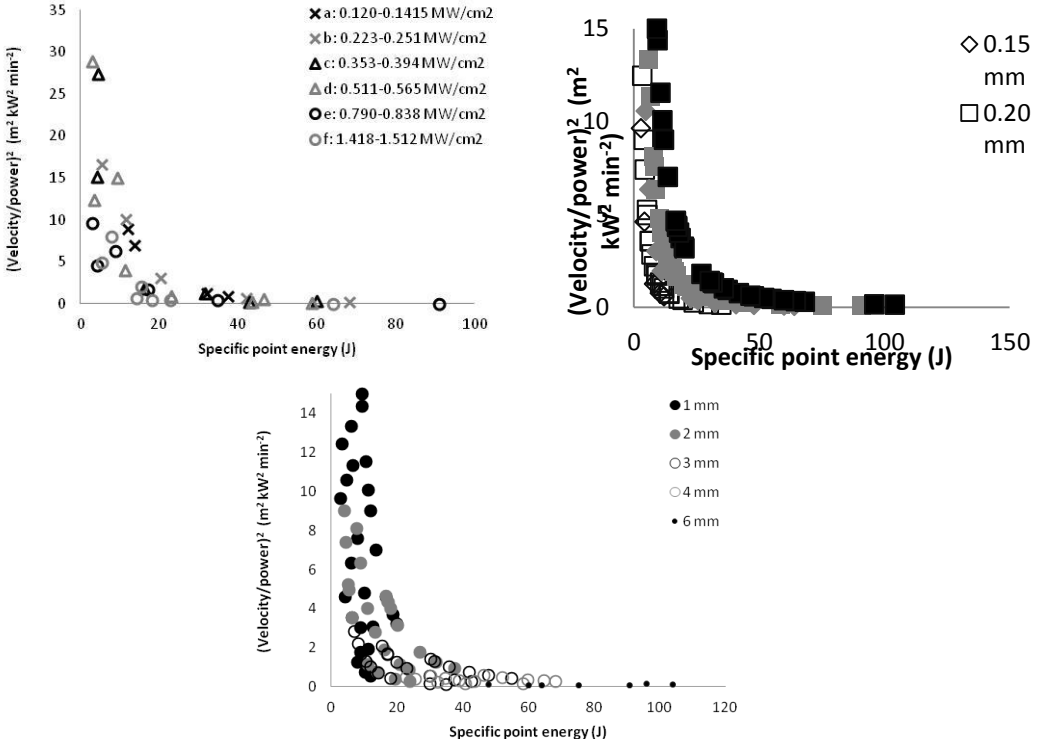

Figure 10 Laser cutting optimisation parameter $(velocity/power)^2$ plotted against SPE, (a) data markers indicate power density (b) data markers indicate beam diameter (c) data markers indicate material thickness.

Figure 10 shows that the laser cutting optimisation parameter increases as specific point energy decreases. Whilst there is scatter within the results it can be said that the gradient of the graph increases at lower SPE values, indicating the greater sensitivity and greater gains that can be achieved by decreasing already small SPE values. It can be again seen (Figure 10b) that the results fall on distinct lines depending on beam diameter, with larger beam diameters being a more optimal choice for any given SPE value. This apparent desirability of larger beam diameters may at first seem counter intuitive however it needs to be noted that this is for the cased of fixed SPE, so any change of beam diameter would not be done in isolation, velocity and power and thereby also interaction time would all also change in order to maintain the SPE. The general trend of thinner section sheet having higher values of The Cutting Optimisation Parameter, $(V/P)^2$, (Figure 10c) results directly from the small SPE values that correspond to the cuts carried out in this work on thinner section sheets.

5. Conclusions

From the work carried out here, and using the definitions of cost and efficiency previously stated, the following conclusions can be drawn:

- The specific point energy analysis approach can be applied to laser cutting as well as laser welding.
- In laser cutting cut kerf width is mainly controlled by beam diameter. The cut kerf width is independent of interaction time.
- Cutting efficiency increases with decreasing SPE.
- For a given material thickness, within the range of parameters used here, energy efficiency can be maximized by selecting the largest beam diameter available and then minimising SPE.
- Maximum efficiency laser cutting is achieved when the cutting optimization factor $(V/P)^2$ is maximized (with acceptable cut quality).

Future work will apply SPE analysis to results from different laser systems.

Acknowledgements

The authors would like to thank Dr Ali Khan of TWI Cambridge and John Cocker of Laser Trader for provision of some of the equipment used in this work.

1. Scintilla, L.D. and L. Tricarico, *Experimental investigation on fiber and CO2 inert gas fusion cutting of AZ31 magnesium alloy sheets.* Optics and Laser Technology, 2013. **46**: p. 42-52.
2. Scintilla, L.D. and L. Tricarico, *Fusion cutting of aluminum, magnesium, and titanium alloys using high-power fiber laser.* Optical Engineering, 2013. **52**(7).
3. Scintilla, L.D. and L. Tricarico, *Laser cutting of lightweight alloys sheets with 1 mu m laser wavelength.* High-Power Laser Materials Processing: Lasers, Beam Delivery, Diagnostics, and Applications Ii, 2013. **8603**.
4. Wandera, C., A. Salminen, and V. Kujanpaa, *Inert gas cutting of thick-section stainless steel and medium-section aluminum using a high power fiber laser.* Journal of Laser Applications, 2009. **21**(3): p. 154-161.
5. Biswas, R., A. S. Kuar, S. Sarkar and S. Mitra, *A parametric study of pulsed Nd:YAG laser micro-drilling of gamma-titanium aluminide.* Optics and Laser Technology, 2010. **42**(1): p. 23-31.
6. Kim, C.J., S. K. Kauh, S. T. Ro and J. S. Lee, *Parametric study of the 2-dimensional keyhole model for high-power density welding processes.* Journal of Heat Transfer-Transactions of the Asme, 1994. **116**(1): p. 209-214.
7. Tzeng, Y.F., *Parametric analysis of the pulsed Nd : YAG laser seam-welding process.* Journal of Materials Processing Technology, 2000. **102**(1-3): p. 40-47.
8. Ghosh, S., B.P. Badgujar, and G.L. Goswami, *Parametric studies of cutting zircaloy-2 sheets with a laser beam.* Journal of Laser Applications, 1996. **8**(3): p. 143-148.
9. Lee, C.S., A. Goel, and H. Osada, *Parametric studies of pulsed-laser cutting of thin metal plates.* Journal of Applied Physics, 1985. **58**(3): p. 1339-1343.
10. Naeem, M., M. Matthews, and S. Ingram, *Parametric study of laser cutting of steel using 1.5kW continuous wave Nd : YAG laser*. Icaleo, ed. P. Christensen. Vol. 87. 2000. C152-C158.
11. Riveiro, A., F. Quintero, F. Lusquinos, R. Comesana and J. Pou, *Parametric investigation of CO2 laser cutting of 2024-T3 alloy.* Journal of Materials Processing Technology, 2010. **210**(9): p. 1138-1152.
12. Shariff, S.M., G. Sundararajan, and S.V. Joshi, *Parametric influence on cut quality attributes and generation of processing maps for laser cutting.* Journal of Laser Applications, 1999. **11**(2): p. 54-63.
13. Steen, W.M., *Laser Material Processing*. 2nd ed. 2001, London: Springer-Verlag.

14. Suder, W.J. and S.W. Williams, *Investigation of the effects of basic laser material interaction parameters in laser welding.* Journal of Laser Applications, 2012. **24**(3): p. 032009.
15. Suder, W.J., *Study of fundamental parameters in hybrid laser welding*, in *School of Applied Sciences*. 2011, Cranfield University.
16. Powell, J., S.O. Al-Mashikhi, A.F.H. Kaplan, K.T. Voisey, *Fibre laser cutting of thin section mild steel: An explanation of the 'striation free' effect.* Optics and Lasers in Engineering, 2011. **49**: p. 1069-1075.